# Optical properties of $In_{1-x}Ga_xAs_yP_{1-y}$ from 1.5 to 6.0 eV determined by spectroscopic ellipsometry

S. M. Kelso
*Bell Laboratories, Murray Hill, New Jersey 07974*
*and Xerox Palo Alto Research Center, Palo Alto, California 94304**

D. E. Aspnes and M. A. Pollack†
*Bell Laboratories, Murray Hill, New Jersey 07974*

R. E. Nahory‡
*Bell Laboratories, Holmdel, New Jersey 07733*
(Received 29 June 1982)

We report high-precision pseudodielectric function spectra ellipsometrically measured from 1.5 to 6.0 eV of $In_{1-x}Ga_xAs_yP_{1-y}$ alloys lattice-matched to InP. Analysis of third derivatives numerically calculated from these data yields critical-point energies, broadening parameters, phases, and amplitudes for the valence–conduction-band critical points $E_1$, $E_1+\Delta_1$, $E_0'$, and $E_0'+\Delta_0'$. An observed inversion of the relative strengths of the $E_1$ and $E_1+\Delta_1$ transitions as a function of composition is attributed to the $k$-linear interaction. The phases indicate strong Coulomb interactions for $E_1$ and $E_0'$, without the ambiguities present in the interpretation of electroreflectance spectra. The composition dependence of critical-point energies yields the following bowing parameters for $E_1$, $E_1+\Delta_1$, $\Delta_1$, and $E_0'$: $0.33\pm0.05$, $0.26\pm0.04$, $-0.07\pm0.02$, and $-0.01\pm0.05$ eV, respectively. We discuss our results with the use of the models of Van Vechten and others for the nonlinear variation of energy gaps and spin-orbit splittings with composition. The $E_0'$ structure may contain contributions from both $\Gamma$ and $\Delta$, as observed in Ge and GaAs. We reassign the feature previously attributed to $E_2$ in InP to $E_0'+\Delta_0'$, where $\Delta_0'$ is the spin-orbit splitting of the second conduction band at $k=0$. Our improved methods of analysis allow spectroscopic ellipsometry to be used as a valuable supplement to modulation spectroscopy for the study of interband transitions in solids.

## I. INTRODUCTION AND SUMMARY

The quaternary semiconductor alloys $In_{1-x}Ga_xAs_yP_{1-y}$ lattice-matched to InP are important in the communications industry because the band gap can be tuned with composition over the spectral range that gives the lowest loss and dispersion for optical fibers.[1] In recent years these materials have been studied rather extensively.[2] Several fundamental properties relating to their band structure have been measured, including the fundamental band gap,[3–13] higher-energy direct gaps,[7–9] the conduction-band mass[12–17] and valence-band mass,[11,13] phonon spectra,[18–20] and core-level spectra.[21,22] Experiments relating to optical properties include index of refraction[23] and reflectance[7] spectra and the indices of refraction at the lasing wavelengths.[23–28] In addition, preliminary band-structure calculations[29–31] have been reported.

In this paper we report measurements[32] of the visible–near-ultraviolet optical properties of eleven samples of $In_{1-x}Ga_xAs_yP_{1-y}$ from $y=0$ (InP) to $y=1$ ($In_{0.53}Ga_{0.47}As$). We measured dielectric-function spectra from 1.5 to 6.0 eV using high-precision spectroscopic ellipsometry. To enhance interband critical-point structures, we numerically calculated third derivatives of these spectra. The derivatives show several features in the $E_1$ and $E_2$ spectral regions and are comparable in quality to electroreflectance (ER) spectra. From a detailed analysis of the derivative line shapes we obtained energy thresholds, broadening parameters, phases, and relative amplitudes associated with the critical points. In contrast to all previous modulation spectroscopic work, our linear regression analysis also yields uncertainties of the fitted parameters. The uncertainties establish the capability of the data to determine these parameters.

The experimental and analytical methods we dis-

 

cuss here can obviously be applied to many other semiconductor alloys and materials systems. In comparison with other techniques, we note the following: Because ellipsometry is a contactless measurement, it can be used on any material, at low or high temperatures, in any transparent ambient. Problems associated with Schottky barriers, Ohmic contacts, and electrolytes are therefore eliminated. Line-shape interpretation is simplified because complex prefactors depending on the material optical parameters, interband masses, and electric field inhomogeneities are also eliminated, as are ill-defined baselines and subsidiary (Franz-Keldysh) oscillations in the spectra. This means that less information is obtained than in a modulation experiment, but this information is unambiguous. An optimum approach is to use the dielectric-function-derived results in conjunction with modulation spectra.

Our results should be useful in several areas. Accurate dielectric-function data[33] provide valuable information about electron-hole interactions. Dielectric functions are necessary for a complete interpretation of modulation spectra. Critical-point energies establish points of reference for band-structure calculations.

In Sec. II we describe our experimental technique, and in Sec. III we present and discuss our data. A brief concluding section follows. Our results are summarized as follows:

(i) We have obtained accurate dielectric-function data from 1.5 to 6.0 eV for compositions from $y=0$ to 1.

(ii) The strength of the $E_1$ transition relative to $E_1+\Delta_1$ increases monotonically with decreasing $y$. This change may be qualitatively understood in terms of the $k$-linear interaction.

(iii) We computed third derivatives of the dielectric-function data and analyzed them in detail by fitting to Lorentzian line shapes. In addition to the usual critical-point energies, we obtained broadening parameters and relative amplitudes. Important phase information was obtained directly.

(iv) Analysis of the $E_1$ and $E_1+\Delta_1$ line shapes is consistent with a $3DM_1$ assignment, with relatively strong excitonic effects corresponding to a phase shift of $\sim 60°$.

(v) Changes in the $E_1$ broadening parameter as a function of composition suggest an alloy-disorder interpretation. Quantitative broadening calculations are not available for comparison at this time.

(vi) We measure a bowing parameter of $0.33\pm0.05$ eV for the $E_1$ critical-point energies and $0.26\pm0.04$ eV for $E_1+\Delta_1$. These values are larger than those obtained in recent electroreflectance studies[8,9] but should be more accurate. Our results are discussed in relation to disorder-induced bowing in the Van Vechten—Bergstresser model.[34]

(vii) The negative bowing that we observe for $\Delta_1$ suggests a revised value $K=0.07$ for this alloy series in an empirical model[35] of the nonlinear variation of spin-orbit splittings.

(viii) The "two-thirds" rule ($\Delta_1=\frac{2}{3}\Delta_0$) is not obeyed in $In_{1-x}Ga_xAs_yP_{1-y}$. This is due to the spatial distribution of the electronic wave functions about the atomic cores.

(ix) Line-shape analysis indicates that $E_0'$ may contain both $\Gamma$ and $\Delta$ contributions, as previously observed in Ge and GaAs. A large Coulomb interaction corresponding to a phase shift of $\sim 110°$ is deduced.

(x) On the basis of calculations of the conduction-band spin-orbit splitting $\Delta_0'$, we reassign the feature previously associated with $E_2$ in InP to $E_0'+\Delta_0'$. We find $\Delta_0'\sim 0.26$ eV.

(xi) The observed bowing of $E_0'$ is zero within experimental error. A small or slightly negative bowing parameter for higher-energy gaps is consistent with theoretical expectations.

## II. EXPERIMENT

A series of $In_{1-x}Ga_xAs_yP_{1-y}$ samples was grown by liquid-phase epitaxy at compositions to lattice match the (100) InP substrates and cover the range $y=0$ to 1.[36] Each layer had a thickness $\geq 1$ $\mu$m, which is greater than the penetration depth of light for the spectral range studied (1.5—6.0 eV). The lattice mismatch as determined by x-ray measurements for each sample was always less than 0.15%. The compositions were determined from the x-ray measurements and from room-temperature luminescence spectra[3] and should be accurate to $\Delta x=\pm0.01$, $\Delta y=\pm0.02$. The compositional homogeneity, both lateral and normal to the layers, was also estimated to be within these tolerances. Carrier concentrations $|N_A-N_D|$ were in the $(10^{16}-10^{17})$-cm$^{-3}$ range, which is sufficiently low that visible—near-ultraviolet optical spectra are unaffected by the impurities.[37]

Dielectric function spectra $\epsilon(E)=\epsilon_1(E)+i\epsilon_2(E)$ were measured at room temperature from 1.5 to 6.0 eV using an automatic spectroscopic rotating-analyzer ellipsometer described elsewhere.[38] The full width at half-maximum (FWHM) spectral resolution was 19 Å (25 meV at 4 eV). The samples were mounted in a windowless cell in flowing dry $N_2$ to minimize surface contamination effects. Sur-

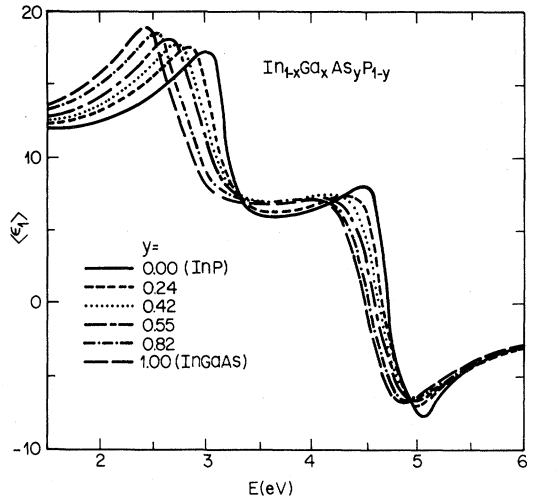


FIG. 1. Real parts $\langle\epsilon_1\rangle$ of pseudodielectric function spectra for compositions of $In_{1-x}Ga_xAs_yP_{1-y}$ lattice-matched to InP.

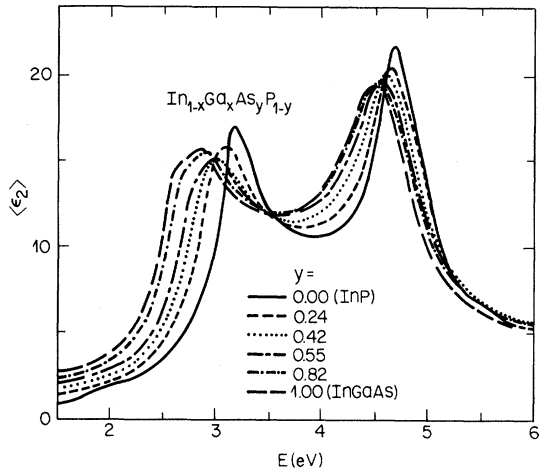


FIG. 2. Imaginary parts $\langle\epsilon_2\rangle$ of pseudodielectric-function spectra corresponding to Fig. 1.

face layers were stripped using a (1:5) solution of HF:methanol or a (1:1) solution of HCl:methanol to obtain a maximum value for the $E_2$ peak in $\epsilon_2$.[39] While the two treatments gave similar results, better (i.e., cleaner and/or smoother) surfaces were obtained using HF:methanol as the final step for samples with $y<0.7$ and HCl:methanol for samples with $y>0.7$. Bromine-methanol chemomechanical polishing procedures[40] were not possible due to the small size of the samples. The surfaces were treated with the samples already optically aligned, and spectra were measured immediately afterward.

## III. RESULTS AND DISCUSSION

### A. Dielectric functions

Real and imaginary parts $\langle\epsilon_1\rangle$ and $\langle\epsilon_2\rangle$ of the complex pseudodielectric functions are shown for selected compositions $y$ in Figs. 1 and 2. Pseudodielectric functions are those calculated from the ellipsometrically measured complex reflectance ratio within the two-phase (substrate-ambient) model without regard to surface overlayers. The differences between these functions and the intrinsic bulk dielectric response should be minor, and will not affect our conclusions based on derivatives of the data. The real and imaginary parts $n$ and $k$ of the complex index of refraction $\tilde{n}=n+ik=(\epsilon_i+i\epsilon_2)^{1/2}$ calculated from Figs. 1 and 2 are shown in Figs. 3 and 4. The two major features of the spectra are the $E_1$ and $E_2$ structures at $\sim 3$ and $\sim 4.5$ eV, respectively. These structures move to lower energy with increasing Ga and As content.

The dominant ($E_2$) peak in $\langle\epsilon_2\rangle$ is highest for InP and $\sim 5-10\%$ lower for other compositions. The decrease for $y\neq 0$ may be intrinsic, e.g., due to alloy disorder or matrix elements, or extrinsic, e.g., due to residual surface overlayers and microroughness. The observed scatter of the $\langle\epsilon_2\rangle$ peak values for different compositions reflects typical differences in sample growth and surface preparation when chemomechanical polishing procedures are omitted. We estimate that our measured $\langle\epsilon_2\rangle$ peaks may be $\sim 5-10\%$ smaller than the true bulk values. Other systematic uncertainties affecting the accuracy of our measurements are discussed elsewhere.[33] The data presented in Figs. 1–4, however, are adequate for most purposes. In the following sections of this paper we use numerically computed third derivatives of these spectra to study interband critical points in the band structure of this alloy system. In addition, the data will be useful in detailed analyses of electroreflectance line shapes.[41]

Our data are in good agreement with those of Burkhard *et al.*[23] where they overlap in energy. This is encouraging, because two different approaches were used. Burkhard *et al.*[23] accepted the presence of oxide overlayers and corrected the data for them. We eliminated the overlayers as much as possible before data acquisition. The former procedure requires some information about oxide thicknesses and assumptions about their interfacial and optical properties for different compositions $y$. The latter procedure supposes that a significant overlayer does not form during the 10 min required to take a spectrum. Studies of Si have shown that

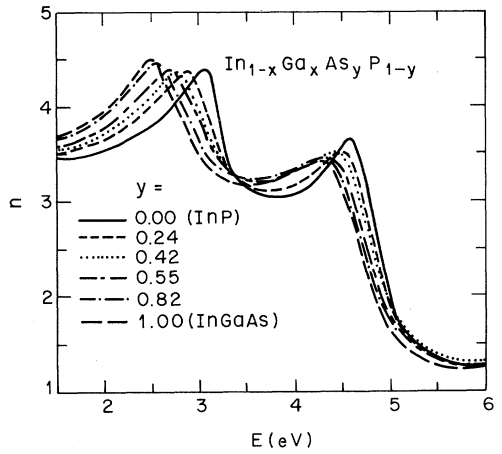


FIG. 3. Real parts $n$ of complex index of refraction spectra for the same samples as in Figs. 1 and 2.

the rate of accumulation of oxide and hydrocarbon contamination overlayers under our experimental conditions is less than 1 Å per hour.[42] The fact that both sides of data agree indicates that both sets of assumptions are valid.

All of the $\langle \epsilon_2 \rangle$ spectra in Fig. 2 have two features in the $E_1$ structure at $\sim 3$ eV, corresponding to the $E_1$ and $E_1+\Delta_1$ transitions between the spin-orbit-split upper valence band and the lowest conduction band along the $\langle 111 \rangle$ direction in the Brillouin zone. It should be noted that the lower ($E_1$) component is stronger in InP ($y=0$) while the upper ($E_1+\Delta_1$) component is stronger in $In_{0.53}Ga_{0.47}As$ ($y=1$). The inversion of the relative strengths of these transitions can be understood in terms of the $k$-linear interaction.[43–46] The intravalence band coupling along $\langle 111 \rangle$ between the upper valence bands causes these bands to repel

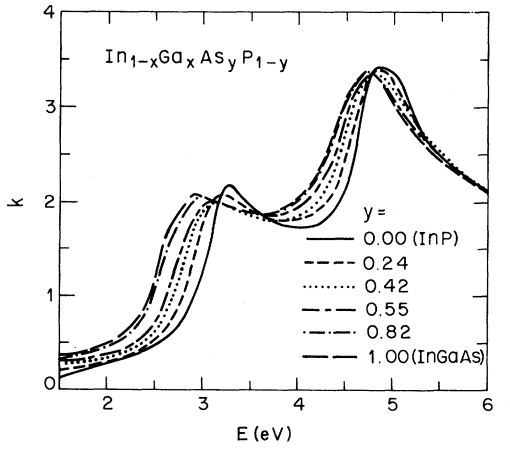


FIG. 4. Imaginary parts $k$ of complex index of refraction spectra corresponding to Fig. 3.

each other in directions perpendicular to $\langle 111 \rangle$. Thus the upper valence band, which gives rise to $E_1$, becomes more nearly parallel to the (lowest) conduction band, while the second valence band, which gives rise to $E_1+\Delta_1$, becomes more curved. This distortion results in an increase in the density of states for $E_1$ at the expense of $E_1+\Delta_1$. The magnitude of the effect depends inversely on the spin-orbit splitting $\Delta_1$, which decreases from $y=1$ to $y=0$. Thus the relative strength of $E_1$ as compared to $E_1+\Delta_1$ is expected to increase with decreasing $y$, as observed in Fig. 2. We note that InP, with the small $\Delta_1$, shows the "anomalous" intensity ratio. Anomalously or vanishingly small $E_1+\Delta_1$ structures are also characteristic of other materials with small $\Delta_1$ spin-orbit splittings, such as GaP (Refs. 37 and 47) and Si.[46]

### B. Third-derivative spectra: $E_1$ and $E_1+\Delta_1$

To study critical-point features in the band structure of these materials, third joint-density-of-states (JDOS) derivatives were computed from the $\langle \epsilon_1 \rangle$ spectra. The original 499-point spectra were smoothed three times by a five-point quadratic routine and contracted to 250 points. The spectra were then differentiated using a seven-point quartic third-derivative routine with coefficients tabulated by Savitzky and Golay.[48] This routine was found to give adequately faithful but smooth derivatives for these samples. Clearly, the appropriate amount of smoothing depends on the width of structures relative to the spacing of data points, as well as on the signal-to-noise ratio of the original spectum. Third derivatives were chosen for improved baseline definition and because the line shapes are related to low-field electroreflectance spectra.[49]

A series of third-JDOS-derivative spectra is shown in Fig. 5 for the energy range 2.0–3.5 eV, which includes the main $E_1$ peak. Both $E_1$ and $E_1+\Delta_1$ features are clearly observed in each spectrum. The original spectra were obtained with sufficient precision ($\delta\epsilon < 5\times 10^{-3}$) to permit noise-free differentiation on this scale. The third-derivative spectra were analyzed by fitting with a theoretical line shape (discussed below) using linear regression analysis[50] to determine the free parameters. The quoted uncertainties represent the 90% confidence level of a statistical analysis and do not include possible systematic errors. The procedure that we use yields more information than the three-point method[51] and another procedure proposed recently.[52]

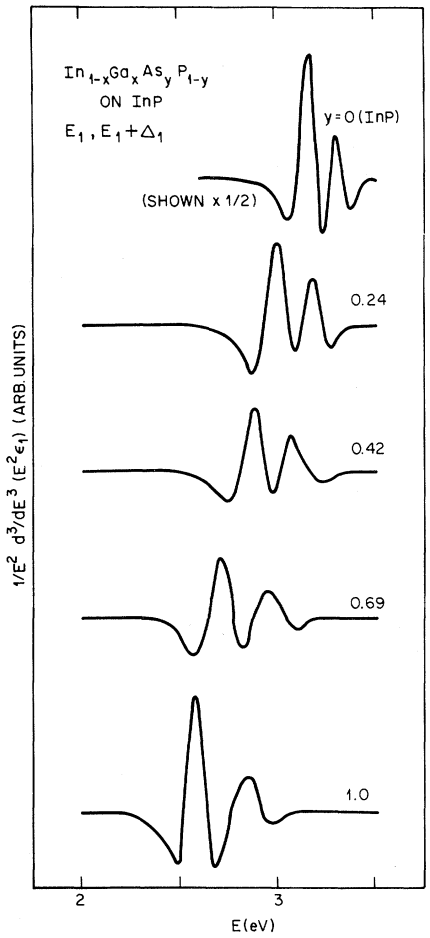


FIG. 5. Third-joint-density-of-states-derivative spectra for $\epsilon_1$ for the spectral range containing the $E_1$ and $E_1+\Delta_1$ transitions.

We assume a simple Lorentzian line shape, which is appropriate for a parabolic density of states[41]:

$$E^{-2}\frac{\partial^3(E^2\epsilon)}{\partial E^3} = ZE^{-2}e^{i[\theta+\pi(j-D)/2]}(E-E_g+i\Gamma)^{-4+D/2} . \quad (1)$$

Here $E_g$ is the critical-point energy, $D$ is the dimension and $j$ the type of the critical point, $\Gamma$ is the broadening parameter, and $Z$ is an amplitude that depends on interband momentum matrix elements. For a simple critical point without excitonic effects, the phase $\theta$ should be zero. Coulomb effects can be described in the contact-exciton approximation[53] by writing[54]

$$\epsilon-1=(\epsilon_0-1)[1+g(\epsilon_0-1)]^{-1} , \quad (2)$$

where $\epsilon_0$ is the dielectric function in the absence of Coulomb effects and $g$ represents the strength of the contact interaction. The third JDOS derivative is given by

$$E^{-2}\frac{\partial^3(E^2\epsilon)}{\partial E^3}=[1+g(\epsilon_0-1)]^{-2}E^{-2}\frac{\partial^3(E^2\epsilon_0)}{\partial E^3} \quad (3)$$

to first order in $g$. If the electron-hole interaction is attractive, i.e., $g<0$, then the (complex) prefactor in Eq. (3) will have a positive phase. From Eq. (1), this is approximately equivalent to obtaining $\theta>0$ from a fit with $g=0$. The same line-shape change also occurs for the case of $\theta=0$ and $g=0$ by increasing $j$. Thus the Coulomb interaction causes a type $M_j$ critical point to look like a mixture of types $M_j$ and $M_{j+1}$.[53] It is expected that the contact interaction may no longer be appropriate for phase shifts as large as $\pi/2$, which corresponds to complete admixture of $M_{j+1}$.

The phase contains information about both the critical-point type and the strength of excitonic effects. Phase analyses have been attempted for electroreflectance spectra of Ge (Refs. 54 and 55) and wavelength-modulated reflectance spectra of InSb.[56] However, the electroreflectance line shape corresponding to Eq. (1) contains complex prefactors that depend on the bulk optical constants and on possible inhomogeneities in the electric field. These prefactors are not always well determined for the case of interest. Direct analysis of the dielectric-function derivatives avoids these ambiguities.

The upper spin-orbit-split valence bands and the lower conduction band are nearly parallel along the $\langle 111\rangle$ direction in zinc-blende semiconductors.[57] If the bands were strictly parallel along $\langle 111\rangle$, $E_1$ and $E_1+\Delta_1$ would be (two-dimensional) 2D-$M_0$ critical points. However, the conduction band actually curves downward slightly relative to the valence bands.[58,59] Thus an alternate description is 3D-$M_1$ (hyperbolic) critical points. In the absence of excitonic effects, a fit to a derivative dielectric-function spectrum would immediately distinguish between these two cases. No other critical-point types are expected in this spectral region for $In_{1-x}Ga_xAs_yP_{1-y}$.

For concreteness consider the spectrum for InP in Fig. 5, which was fit to two structures given by Eq. (1). $Z$, $E_g$, $\Gamma$, and $\theta$ were the free parameters for each structure, except that the two phases were constrained to be equal. We found $\theta=106°\pm4°$ for a 2D-$M_0$ critical point and $\theta=57°\pm5°$ for a 3D-$M_1$ critical point. If $\theta<\pi/2$, then the $E_1$ and $E_1+\Delta_1$ structures are more appropriately identified as

3D-$M_1$ critical points with the Coulomb interaction giving rise to the 57° phase shift. This is consistent with the earlier results[54–56] on other materials. The mean-square deviation of the fitted curve is larger for 3D-$M_1$ than for 2D-$M_0$. This is a result of a poorer fit in the wings of the spectrum, probably due to nonparabolicity in the actual density of states.[60] We did not attempt to fit more complicated line shapes. The relatively large phase shift resulting from the Coulomb interaction is also consistent with one-electron calculations of $\epsilon_2$ in similar materials, which underestimate measured strengths for the $E_1$ and $E_1+\Delta_1$ peaks by $\sim 25-40\%$.[59,61,62] An appropriate increase in $\epsilon_2$ can be obtained by using $g \neq 0$ in the prefactor of Eq. (2). For example, for $E_1$ ($E=3.16$ eV, where $\langle \epsilon_1 \rangle = 11.82$ and $\langle \epsilon_2 \rangle = 16.94$), $g=-0.024$ gives a phase shift of 57° and an 18% correction to the $\epsilon_2$ peak height. We note that $\theta$ was $\sim 20°-30°$ smaller for the other compositions.

In Fig. 5, the peak-to-peak height of the InP derivative is much greater than those of the other spectra, and the linewidth is noticeably narrower. However, the strength of a feature is not given by the peak-to-peak height of the derivative spectrum, but rather by the amplitude $Z$ in Eq. (1). From our analysis of all the spectra we find that the strength of the $E_1$ transition decreases with increasing $y$ for $y<0.6$ and then increases slightly. The minimum value of $Z(E_1)$ is slightly over half that of InP. If we interpret the overall decrease in $Z$ as a reduction in excitonic effects, then we obtain qualitative agreement with the trend for $\theta$.

The ratio $Z(E_1+\Delta_1)/Z(E_1)$ increases smoothly from $\sim 0.5$ for InP to $\sim 1.1$ for $In_{0.53}Ga_{0.47}As$. Although the statistical uncertainties are large, $\sim 30\%$, and a ratio larger than 1.0 may be unphysical, the trend is clear. As mentioned in the previous section with regard to the $\langle \epsilon_2 \rangle$ spectra, it can be qualitatively understood in terms of the $k$-linear interaction. We performed a numerical calculation[46] of the above ratio using values of matrix elements similar to those appropriate for Si (Refs. 44 and 46) and GaAs.[45] We could not reproduce such a large change in the amplitude ratio between $y=0$ and $y=1$ keeping the matrix elements constant. This is probably due to approximations in the calculation which do not represent the band structure sufficiently accurately.

As noted above, the $E_1$ and $E_1+\Delta_1$ features are narrowest in InP: We find $\Gamma = 64 \pm 2$ and $63 \pm 5$ meV, respectively. For the $E_1$ transitions, $\Gamma$ increases with $y$ to a maximum value of $\approx 110$ meV for $y \approx 0.6$, then decreases to $87 \pm 5$ meV for $y=1$. A likely origin of the increase in $\Gamma$ is potential fluctuations resulting from random atomic placement in the alloys. In principle there are different contributions from disorder on the cation and anion sublattices. The maximum anion disorder occurs at $y=0.5$ while that for cation disorder occurs at $x=0.5$ or $y=1$. This suggests that the primary origin of the variation in $\Gamma(E_1)$ is anion disorder. The relatively small value of $\Delta_1$ (see Sec. III C) also indicates a large anion influence in this part of the Brillouin zone. Studies on pseudobinary alloys such as $Al_xGa_{1-x}As$ or $GaAs_{1-x}P_x$, which contain only one type of sublattice disorder, should help identify these contributions. In general, alloy disorder is expected to broaden optical spectra. In one approach to this problem, the broadening of exciton states arises primarily from the variation of threshold energies due to fluctuations in composition.[63–65] However, the resulting values ($<1$ meV for III-V materials) are much too small to explain our observations. In another approach, a lifetime broadening is expressed as twice the imaginary part of complex energy bands.[66] Although quantitative estimates have not been given, the broadening is predicted to vary with position in the Brillouin zone.

We found that the broadening parameter for $E_1+\Delta_1$ increases monotonically with $y$ by approximately a factor of 2 to $126 \pm 15$ meV for $y=1$. A larger broadening for $E_1+\Delta_1$ could result because the $E_1+\Delta_1$ hole is in a state that can decay more readily than the $E_1$ hole. This effect should be greater in materials with larger $\Delta_1$. We observe ratios[37] $\Gamma(E_1+\Delta_1)/\Gamma(E_1)$ of $86/63=1.4$ and $100/83=1.2$ for GaAs and Ge, respectively, both of which have spin-orbit splittings and $E_1$ gaps similar to $y=1$.

### C. Critical-point energies, bowing: $E_1$ and $E_1+\Delta_1$

For InP, the fit to our experimental third-derivative spectrum yields $E_1 = 3.158 \pm 0.004$ eV, $E_1+\Delta_1 = 3.291 \pm 0.004$ eV, and $\Delta_1 = 0.133 \pm 0.004$ eV. These values are in reasonable agreement with those obtained from electroreflectance[8,9,67] and wavelength-modulated reflectance[68,69] measurements. The present values should be more accurate: The electroreflectance line shapes were apparently not analyzed quantitatively, and first-derivative spectra have less well-defined features than third-derivative spectra. In this regard, we also note that the common practice of associating critical-point energies with peaks in normal-incidence reflectance[7] or $\epsilon_2$ (Ref. 23) spectra is particularly dangerous and

can give substantial errors (as much as 0.1 eV, depending on the linewidth). Indeed, only one peak is resolved for $E_1$ and $E_1+\Delta_1$ in this alloy series (see Fig. 2); and this peak is related to $E_1$ for InP and to $E_1+\Delta_1$ for $In_{0.53}Ga_{0.47}As$.

Our results for $E_1$ and $E_1+\Delta_1$ are shown as a function of alloy composition in Fig. 6. As anticipated from Figs. 1–4, the critical-point energies decrease with increasing $y$. The spin-orbit splitting increases to $\Delta_1=0.259\pm0.013$ eV in $In_{0.53}Ga_{0.47}As$, where $E_1=2.570\pm0.007$ eV and $E_1+\Delta_1=2.829\pm0.006$ eV. These critical-point energies are in remarkably good agreement with the results of two early electroreflectance studies on $In_{1-x}Ga_xAs$ alloys,[70,71] although only qualitative line-shape analyses were performed at that time. The spin-orbit splitting may be expected to increase with increasing $y$ because of the larger values of $\Delta_1$ observed[37] in both GaAs ($0.224\pm0.006$ eV) and InAs ($0.274\pm0.008$ eV). Indeed, a simple linear interpolation predicts $\Delta_1=0.251\pm0.010$ eV for $In_{0.53}Ga_{0.47}As$.

The variations with composition of the $E_1$ and $E_1+\Delta_1$ critical-point energies are expected, as in other III-V semiconductor alloys,[72] to be quadratic:

$$E(y)=A+By+Cy(y-1)\,. \tag{4}$$

Here $A=E(0)$ and $B=E(1)-E(0)$, while $C$ is a bowing parameter. The critical-point energies obtained from our line-shape analysis were fit to Eq. (4). The results are shown as the solid curves in Fig. 6 and are listed with uncertainty estimates in Table I. Because all three coefficients were fitted parameters, the energies at $y=0$ and 1 from Eq. (4) and Table I are slightly ($\lesssim 5$ meV) different from those stated earlier in this section. Our preliminary

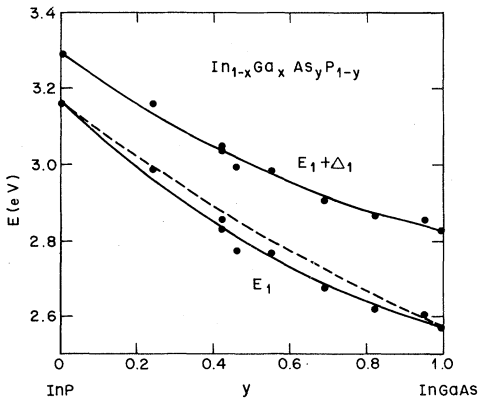


FIG. 6. Critical-point energies $E_1$ and $E_1+\Delta_1$ as a function of composition $y$, as obtained from line-shape fits. Curves are discussed in the text.

analysis[21] yielded the same result for $C(E_1)$ but a smaller value for $C(E_1+\Delta_1)$. This difference arises from fitting the two phases independently [see Eq. (1)] in the earlier analysis but constraining the phases here to be the same. If the two critical points are of the same type, then the present approach is more nearly correct, for a moderate electron-hole interaction strength $g$ in Eq. (2). A three-point line-shape analysis[51] is not accurate when the lines overlap, as they do here. It was suggested in early work[35,73] that the $E_1$ and $E_1+\Delta_1$ critical points are located at slightly different points in the Brillouin zone, but we know of no evidence from recent data or band-structure calculations to support this hypothesis.

The bowing parameters listed in Table I are larger than those obtained by analysis of electroreflectance data.[8,9] Part of the difference may arise from systematic differences in line-shape analysis. When we fit the positive peaks of our third-derivative spectra to Eq. (4), we obtained bowing parameters smaller than the tabulated values by 0.05 eV. Apparently, more serious systematic discrepancies are present. We note that our bowing parameter for $E_1$ is in good agreement with that obtained from an interpolation formula,[9] but that a similar interpolation formula[3,74] overestimated the measured deviation from linear behavior for $E_0$ by a factor of 2.[3]

It has long been recognized that band-gap bowing in semiconductor alloys results from at least two contributions. The first arises from the virtual-crystal approximation, in which the magnitude of the periodic crystal potential and the lattice constant vary linearly with composition, and can give upward or downward bowing. The second is due to disorder on one of the sublattices (cation or anion) and always results in downward bowing for the lowest gaps. Each contribution has been estimated using several different models.[34,66,73,75–78] However, it has been noted[11,79] that the contribution due to the change in lattice constant should be strictly zero in $In_{1-x}Ga_xAs_yP_{1-y}$ due to the lattice-matched condition. The second term is more complicated here than for pseudobinary alloys, since disorder exists on both sublattices. Using a Van Vechten–Bergstresser approach,[34] Pearsall[79] has estimated that the term $Cy(y-1)$ in Eq. (4) becomes $-0.07y+0.15y(y-1)$ eV. The magnitude of the quadratic term agrees well with that obtained from the electroreflectance studies[8,9] and is therefore smaller than ours.[80] The dashed curve in Fig. 6 is calculated from Eq. (4) with $C=0.15$ eV and our values for $A$ and $B$. It is clear that the data are

TABLE I. Fitted values for quadratic variation of energies.

| Energy | Data source | $A$ (eV) | $B$ (eV) | $C$ (eV) |
|---|---|---|---|---|
| $E_1$ | Critical point | 3.163±0.013 | −0.590±0.016 | 0.33±0.05 |
| $E_1+\Delta_1$ | Critical point | 3.296±0.010 | −0.466±0.013 | 0.26±0.04 |
| $\Delta_1$ | | 0.133±0.005 | 0.124±0.007 | −0.07±0.02 |
| $E_0'$ | Peak | 4.72 ±0.01 | −0.31 ±0.02 | −0.01±0.05 |

not well described by this curve.

Our experimental values for $\Delta_1$ are shown as a function of composition in Fig. 7. The relatively low scatter in the data was achieved by constraining the phases of the $E_1$ and $E_1+\Delta_1$ line shapes to be equal and thereby eliminating a major source of spurious scatter. A fit to Eq. (4) with the coefficients $A$, $B$, and $C$ given in Table I is shown as the solid curve in the figure. We find a bowing parameter $C(\Delta_1)=-0.07\pm0.02$ eV. This negative or upward bowing of $\Delta_1$ was also observed in the electroreflectance studies,[8,9] as well as for many pseudobinary semiconductor alloys.[73,81,82] Van Vechten *et al.*[35] proposed that the deviation from a linear function of composition can be described as follows using second-order perturbation theory:

$$\Delta_1(y)=\Delta_1(0)+by-\frac{aKW}{\Delta_1(0)+by}\ , \tag{5}$$

where $a$ is a bandwidth and $K$ is a constant. The value for $y=1$ determines $b$. For $In_{1-x}Ga_xAs_yP_{1-y}$ the bowing $W$ can be written[79]

$$W=1/a[-0.07y+0.15y(y-1)]\ , \tag{6}$$

as for $E_1$. Van Vechten *et al.*[34,35] suggested that $a\approx0.98$ eV and $K=0.14$ should be universal values for all semiconductor alloys. To examine this hypothesis, we calculated the dashed curve in Fig. 7 with this value for $K$ [$a$ drops out of Eq. (5)]. The result does not fit the data well. Since the original values for $a$ and $K$ were each chosen to fit another alloy system and since their universality does not seem to be substantiated, we determined new values to fit our data for $In_{1-x}Ga_xAs_yP_{1-y}$. From the $\Delta_1$ data we find $K=0.075$, which gives the dotted-dashed curve in Fig. 7. This curve is nearly indistinguishable from the simple quadratic form and fits the data very well. If we then use $C=0.15/a$ from Eq. (6) in Eq. (4) for $E_1$, we obtain $a=0.45$ eV and the solid curve in Fig. 6 is retained. In support of our revised value for $K$, we note that it would provide excellent agreement with the $In_{1-x}Ga_xAs$ data quoted by Van Vechten *et al.*[35] In any case, this model is empirical. A more quantitative calculation of $\Delta_1$ using, for example, tight-binding methods[83] would be complicated and is not presently available.

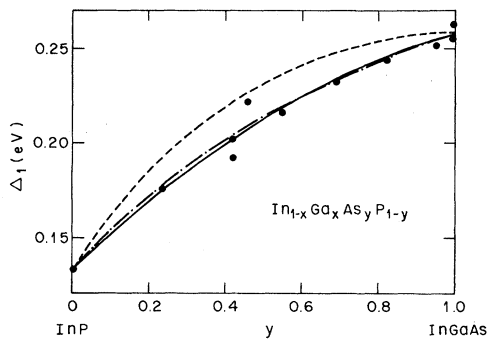


FIG. 7. Spin-orbit splitting $\Delta_1$ vs composition. Curves are discussed in the text.

Because the $k$-linear interaction affects the relative intensities of the $E_1$ and $E_1+\Delta_1$ structures in InP, we checked to see if it also affects their threshold energies, and therefore the apparent value of $\Delta_1$. If so, the true value of $\Delta_1$ in InP would be smaller than the apparent value,[46] and the $y$ dependence would be modified. Our calculations showed that the $E_1$ and $E_1+\Delta_1$ thresholds remain unshifted as a result of the $k$-linear interaction. Thus we anticipate no distortion in Fig. 7 due to this effect.

For binary compounds, the $\frac{2}{3}$-rule[67,84] has been used to relate the value of $\Delta_1$ to that of $\Delta_0$ according to $\Delta_1=\frac{2}{3}\Delta_0$. This rule is obeyed fairly accurately in materials for which the atomic spin-orbit splittings of the constituents are not too different[83]; this usually means that the cation and anion come from the same row of the Periodic Table.[67] It is well known that the data for InP cannot be described by this rule or by any other simple empirical[67] or tight-binding[83] calculation: Experimentally, $\Delta_0=0.11$ eV (Refs. 8, 9 and 67) and $\Delta_1=0.133$ eV so that $\Delta_1\approx1.2\Delta_0$. Both InAs and GaAs are more "normal," with $\Delta_1=0.25$ eV$\approx0.58\Delta_0$ and $\Delta_1=0.22$ eV$\approx0.66\Delta_0$, respectively. A prediction for $In_{0.53}Ga_{0.47}As$ is complicated by the different quadratic composition dependences of $\Delta_0$ and $\Delta_1$ due to

alloy disorder.[35] Experimentally $\Delta_0 \approx 0.34$ eV (Refs. 8 and 9) and $\Delta_1 = 0.257$ eV so that $\Delta_1 \approx 0.76\Delta_0$. Thus a smooth decrease in $\Delta_1/\Delta_0$ from 1.2 to 0.76 is expected and observed[8,9] as $y$ increases from 0 to 1.

As discussed above, calculations of the effect of alloy disorder on critical-point energies predict quadratic dependences on alloy composition. For example, this means that the $E_1$ gap is reduced in $In_{0.53}Ga_{0.47}As$ as a result of the *random* placement of In and Ga atoms on the cation sublattice. Thus $E_1$ should increase if the In and Ga atoms were arranged *periodically* on the cation sites. Ignoring for a moment the difference between $In_{0.53}Ga_{0.47}As$ and $In_{0.50}Ga_{0.50}As$, this situation could in principle be realized in an $InGaAs_2$ chalcopyrite-type crystal structure or in a superlattice consisting of alternating layers of InAs and GaAs. The latter structure could actually be grown using state of the art molecular-beam epitaxy techniques. A study of such a material would provide an interesting test of theories of the effects of disorder on band structure.

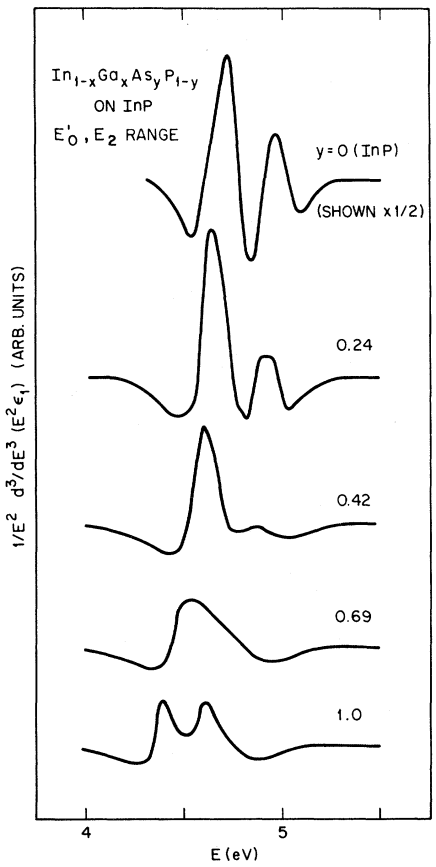


FIG. 8. Third-joint-density-of-states-derivative spectra for $\epsilon_1$ for the spectral range containing $E_0'$- and $E_2$-related transitions.

For this example, the shift in $E_1$ would be $\sim 70$ meV for $a = 0.98$ eV in Eq. (6) or $\sim 155$ meV for our value $a = 0.45$ eV. A shift of this magnitude would be readily observable.

### D. The $E_2$ spectral range

Figure 8 shows third-derivative spectra for the energy range 4.0–5.5 eV, which includes the dominant $E_2$ peak in the $\langle \epsilon_2 \rangle$ spectra. Here, the assignment of features is less certain than for Fig. 5. We expect to observe features corresponding to the following transitions: $E_0'$, between the upper valence band and the lower (singlet) component of the second conduction band at or near $\Gamma$; $E_0' + \Delta_0'$, between the upper valence band and the upper (doublet) component of the second conduction band also at or near $\Gamma$; $E_2$, between the upper valence and lower conduction bands along $\Sigma$ [(110) direction] or near $X$; and subsidiary structures $E_2 + \delta$ or $E_2 + \Delta_2$. Our experimental spectra do not show all of these features. Of necessity, then, our analysis will be less complete than that for the $E_1$ spectral range.

In an electroreflectance experiment,[67] the structure near 4.7 eV in InP has been associated with $E_0'$. It clearly has a counterpart in all the spectra for other compositions, shifting smoothly to $\sim 4.4$ eV in $In_{0.53}Ga_{0.47}As$. We begin by accepting this assignment. If the transition occurs at $\Gamma$, then the critical point should be of the 3D-$M_0$ type. A fit of our spectrum for InP to Eq. (1) yields the following parameters: $E_0' = 4.728$ eV, $\Gamma(E_0') = 130$ meV, and $\theta = 150°$. However, detailed analyses of low-temperature electroreflectance measurements of Ge (Refs. 85 and 86) and GaAs (Ref. 87) show that $E_0'$ can contain contributions from two different types of critical points. In GaAs, in addition to the expected 3D-$M_0$ critical point $E_0'(\Gamma)$ at or nearly at[88] $\Gamma$, there is a second set of critical points $E_0'(\Delta)$ of type 3D-$M_1$ with approximately equal combined strength occurring between the same two bands but located along $\langle 100 \rangle$ about 10% of the way to $X$. The separation between $E_0'(\Gamma)$ and $E_0'(\Delta)$ was found to be $\sim 40-50$ meV in GaAs, with the $\Delta$ point lying higher in energy.[87] Accordingly, we tried representing a 3D-$M_0$ line shape with $\Gamma = 130$ meV and $\theta = 150°$ by a sum of 3D-$M_0$ and 3D-$M_1$ line shapes with equal intensities, broadening parameters, and phases, and a separation to be determined. We obtained a reasonable representation for $\Gamma \approx 120$ meV, $\theta \approx 110°$, and a separation of $\sim 120$ meV. The primary difference between the two representations was that the two-line spectrum

showed slightly deeper dips in the wings, a feature also exhibited by the experimental spectrum. Thus our data are consistent with the following assignments: $E_0'(\Gamma)=4.67\pm0.01$ eV, $E_0'(\Delta)=4.79\pm0.01$ eV, $\Gamma(E_0')=120\pm10$ meV, and $\theta=110°\pm10°$.

If this assignment is correct, electroreflectance spectra of the $E_0'$ region in InP should also exhibit an anomalous polarization dependence. In addition, the two components should be resolvable in low-temperature spectra either in electroreflectance or ellipsometry. The large value for the phase is somewhat surprising. However, we note that a 2D-$M_0$ analysis[86] of the $\Gamma$ transition in Ge gave $\theta\approx75°$, which is equivalent to $\theta\approx120°$ for 3D-$M_0$. Thus the phase shifts are comparable for these two materials. The phase shift was attributed previously[86] to the Coulomb interaction, although there is actually no unambiguous evidence for this. We do not know the reason for the large broadening parameter, as compared to that for $E_1$; at room temperature, the largest contribution should be temperature.

Possible assignments for the upper InP structure in Fig. 8 depend on the value of $\Delta_0'$. Some confusion is possible, since the definitions of both $E_0'$ and $\Delta_0'$ have changed with time. In the early electroreflectance work,[67] $E_0'$ was believed to be $E_0'(\Delta)$, and $E_0'+\Delta_0'$ was taken to be the transition to the same (singlet) conduction band but originating from the lower member of the upper valence band separated by the valence-band spin-orbit splitting along $\langle 100\rangle$, then labeled $\Delta_0'$. The assignment appeared verified when two structures separated by 70 meV were suggested by the electroreflectance spectrum, since this separation was in good agreement with a calculation of the valence-band splitting along $\langle 100\rangle$. (However, it is stated elsewhere in the same paper that a spin-orbit splitting of 0.1 eV was too small to be resolved.) A later low-temperature wavelength-modulated reflectance spectrum[69] and spectra for other materials[67,69,89] were similarly interpreted in terms of $E_0'(\Delta)$ and its valence-band spin-orbit-split partner. If such resolution is indeed possible at 80 K in a first-derivative spectrum, we suggest that the two structures actually correspond to $E_0'(\Gamma)$ and $E_0'(\Delta)$ and have no connection to spin-orbit splittings. In fact, subsequent polarization-dependent and stress experiments on Ge (Refs. 85, 86, 90, and 91) and GaAs (Ref. 87) showed persuasively that transitions at $\Gamma$ were dominant for $E_0'$ and that the structure labeled $E_0'+\Delta_0'$ was related to $E_0'$ by the spin-orbit splitting of the second conduction band at $\Gamma$. Since then, the association of $\Delta_0'$ with the spin-orbit splitting of the second conduction band at $\Gamma$ seems to have been accepted to such an extent that it is not stated explicitly.

With the present definition, $\Delta_0'$ for InP should be much larger than the spin-orbit splitting of the valence band along $\langle 100\rangle$, which we shall call $\Delta_{100}$. The reason is simple: In an ionic material the electronic states have relatively pure cation or anion character at $\Gamma$. Thus, just as the valence-band spin-orbit splitting $\Delta_0$ in zinc-blende materials is determined primarily by the anion atomic spin-orbit splitting, the conduction-band spin-orbit splitting $\Delta_0'$ is determined primarily by the cation atomic spin-orbit splitting.[92] Chadi's tight-binding calculation[83] gave $\Delta_0'=0.31$ eV for InP, while Chelikowsky and Cohen's pseudopotential band-structure calculation[59] gave $\Delta_0'=0.28$ eV. The $\vec{k}\cdot\vec{p}$ calculation of Cardona *et al.*[67] gave $\Delta_{15}=0.74$ eV (in the old notation), but the $\vec{k}\cdot\vec{p}$ calculation probably overestimates this spin-orbit splitting by a factor of 2.[93] These theoretical considerations suggest that the upper structure in InP, previously[67] assigned to $E_2$, is actually $E_0'+\Delta_0'$. This critical point is at or nearly at $\Gamma$ and does not have an associated critical point along $\langle 100\rangle$. Note that this interpretation is qualitatively different from that of the previous electroreflectance analysis of GaAs (Ref. 87), where a $\Delta$ contribution was also found near $E_0'+\Delta_0'$. This extra contribution would involve the lower member of the spin-orbit-split valence band along $\langle 100\rangle$ and the lower conduction band, occurring at this energy because $\Delta_0'$ and $\Delta_{100}$ are similar in GaAs. In InP, however, this extra contribution would be very close to $E_0'(\Delta)$, since $\Delta_{100}$ is expected to be $<100$ meV.[67] In support of our interpretation, we note that the fit yielded a phase $\theta=103°\pm10°$ for a 3D-$M_0$ line shape for $E_0'+\Delta_0'$, nearly identical to the phases of $E_0'(\Gamma)$ and $E_0'(\Delta)$, as expected for related critical points. On the other hand, the phase of $E_2$ in other materials where the identification is unambiguous (Ge, GaP, GaAs, GaSb, and InSb) is considerably larger.[37] Our analysis gives $\Delta_0'=0.26\pm0.02$ eV, in good agreement with the calculations.

We also associate the upper structure in the $y=1$ spectrum with $E_0'+\Delta_0'$. In this case we find $\Delta_0'\approx0.20$ eV. For comparison, $\Delta_0'$ in GaAs is[87] 0.175 eV while theoretical estimates[59,83] are 0.16 or 0.24 eV. For InAs, experimental estimates[67,69–71,89] range from 0.10 to 0.28 eV, while calculations[59,83] show 0.26 and 0.40 eV. In the experiments[67,71] yielding the largest value, it was proposed that the $E_0'+\Delta_0'$ and $E_2$ structures coincide. Because of the relatively large intensity of the upper structure in $In_{0.53}Ga_{0.47}As$, we should not rule out a similar overlap and hence a double assignment of $E_0'+\Delta_0'$

and $E_2$. An electroreflectance spectrum from a bulk polycrystalline sample of similar composition ($In_{0.55}Ga_{0.45}As$) showed a feature near the upper structure of Fig. 8 but nothing corresponding to the lower structure.[71]

In many semiconductor-alloy systems, the study of systematic variations with composition aids greatly in the identification of spectral features. The curves in Fig. 8 indicate, however, that $In_{1-x}Ga_xAs_yP_{1-y}$ may be an exception in the $E_2$ spectral range. We note first that we never resolve more than two of the three most prominent expected features ($E_0'$, $E_0'+\Delta_0'$, $E_2$). Thus we have either overlapping or "missing," i.e., weak, structures. In addition, for intermediate compositions $y$, the second feature weakens considerably and almost disappears. Laufer *et al.*[9] apparently observed more structure in their electroreflectance spectra, possibly due to different sensitivities of the critical points to the modulating electric field.

Because of the complexity of the spectra and the smaller peak-to-peak heights (and signal-to-noise ratios) for large $y$, we have not attempted line-shape fits for compositions $y \neq 0$. In Fig. 9 we show the energies corresponding to positive peaks in the third-derivative spectra. This gives a reasonably faithful description of the variations with composition, since the line-shape phase does not change very much across the sequence. We find that for small $y$, $\Delta_0'$ remains approximately constant. As $y$ decreases from 1, $\Delta_0'$ apparently decreases slightly. This trend toward smaller $\Delta_0'$ is expected for intermediate $y$ as a disorder-induced effect.[94] Ambiguity in the $E_0'+\Delta_0'$ vs $E_2$ assignment could be removed in principle by studies of $In_{1-x}Ga_xP$ and $In_{1-x}Ga_xAs$ alloys. Although previous electroreflectance studies[71,82] on these systems were not sufficiently detailed in this spectral range to draw any conclusions, a spectrum[37] for $In_{0.15}Ga_{0.85}As$ supports the double assignment for $y=1$.

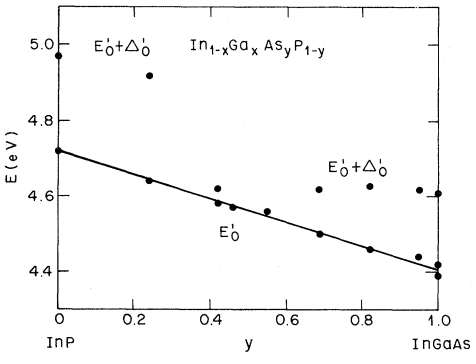


FIG. 9. Peak energies of third-derivative spectra corresponding to Fig. 8. Curve is a fit to Eq. (4).

The peak $E_0'$ energies in Fig. 9 were fit to Eq. (4) to obtain a bowing parameter. As indicated in Table I, we found $C=-0.01\pm0.05$ eV, i.e., zero within experimental uncertainty. This value is smaller than that found for the $E_0$ or $E_1$ transitions. If there is a phase variation with composition similar to $E_1$, then $C$ could be reduced by $\sim 0.05$ eV to $\sim -0.06$ eV. It has been suggested[34,73] that the bowing due to alloy disorder should be roughly the same for transitions between the same bands even at different points in the Brillouin zone, because the disorder is a spatially localized fluctuation. Another calculation[75] suggests a negative bowing parameter for large gaps. Our observation of nearly zero or slightly negative bowing for $E_0'$ supports the latter idea.

## IV. CONCLUSIONS

We have shown that spectroscopic ellipsometry is a useful tool for obtaining detailed information about interband critical points as well as accurate optical constants. In applying new methods of analysis specifically to $In_{1-x}Ga_xAs_yP_{1-y}$ alloys lattice-matched to InP, we found that the $k$-linear interaction could qualitatively explain the observed relative intensity changes in the $E_1$ and $E_1+\Delta_1$ transitions. Phases extracted from line-shape analyses indicated strong Coulomb or excitonic effects. We revised the previously accepted assignment of $E_2$ to $E_0'+\Delta_0'$ in InP. In addition, we have obtained improved values for the bowing parameters of the $E_1$, $E_1+\Delta_1$, and $E_0'$ transitions and the $\Delta_1$ spin-orbit splitting. The bowing parameters were discussed in terms of the Van Vechten—Bergstresser model of alloy disorder.

## ACKNOWLEDGMENTS

We would like to thank J. C. DeWinter for assistance in the preparation of the samples, D. J. Chadi for helpful discussions, and M. Cardona for comments on the manuscript.

*Present address.
†Present address: Bell Laboratories, Crawford Hill Laboratory, Holmdel, New Jersey 07733.
‡Present address: Bell Laboratories, Murray Hill, New Jersey 07974.

[1]T. Miya, Y. Terunuma, T. Hosaka, and T. Miyashita, Electron. Lett. 15, 106 (1979); K. I. White and B. P. Nelson, *ibid.* 15, 396 (1979).
[2]See *GaInAsP Alloy Semiconductors,* edited by T. P. Pearsall (Wiley, Chichester, 1982).
[3]R. E. Nahory, M. A. Pollack, W. D. Johnston, Jr. and R. L. Barns, App. Phys. Lett. 33, 659 (1978).
[4]Y. Takeda, A. Sasaki, Y. Imamura, and T. Takagi, J. Appl. Phys. 47, 5405 (1976).
[5]K. Nakajima, A. Yamaguchi, K. Akita, and T. Kotani, J. Appl. Phys. 49, 5944 (1978).
[6]Y. Yamazoe, H. Takakura, T. Nishino, Y. Hamakawa, and T. Kariya, J. Cryst. Growth 45, 454 (1978); Y. Yamazoe, T. Nishino, Y. Hamakawa, and T. Kariya, Jpn. J. Appl. Phys. 19, 1473 (1980); Y. Yamazoe, T. Nishino, and Y. Hamakawa, IEEE J. Quant. Elec. QE-17, 139 (1981).
[7]H. H. Caspers and H. H. Wieder, Solid State Commun. 29, 403 (1979).
[8]E. H. Perea, E. E. Mendez, and C. G. Fonstad, Appl. Phys. Lett. 36, 978 (1980).
[9]P. M. Laufer, F. H. Pollak, R. E. Nahory, and M. A. Pollack, Solid State Commun. 36, 419 (1980).
[10]S. N. Grinyaev, M. A. Il'in, A. I. Lukomskii, V. A. Chaldyshev, and V. M. Chupakhina, Fiz. Tekh. Poluprovodn. 14, 760 (1980) [Sov. Phys.—Semicond. 14, 446 (1980)].
[11]C. Hermann, G. Lampel, and T. P. Pearsall, in Proceedings of the Fifteenth International Conference on the Physics of Semiconductors, Kyoto, 1980 [J. Phys. Soc. Jpn. 49, Suppl. A, 631 (1980)]; C. Hermann and T. P. Pearsall, Appl. Phys. Lett. 38, 450 (1981).
[12]T. Nishino, Y. Yamazoe, and Y. Hamakawa, Appl. Phys. Lett. 33, 861 (1978).
[13]K. Alavi, R. L. Aggarwal, and S. H. Groves, J. Magn. Magn. Mater. 11, 136 (1979); Phys. Rev. B 21, 1311 (1980).
[14]J. B. Restorff, B. Houston, J. R. Burke, and R. E. Hayes, Appl. Phys. Lett. 32, 189 (1978); J. B. Restorff, B. Houston, R. S. Allgaier, M. A. Littlejohn, and S. B. Phatak, J. Appl. Phys. 51, 2277 (1980).
[15]R. J. Nicholas, J. C. Portal, C. Houlbert, P. Perrier, and T. P. Pearsall, Appl. Phys. Lett. 34, 492 (1979); J. C. Portal, P. Perrier, M. A. Renucci, S. Askenazy, R. J. Nicholas, and T. P. Pearsall, in *Physics of Semiconductors 1978,* edited by B. L. H. Wilson (IOP, London, 1979), Vol. 43, p. 829; R. J. Nicholas, S. J. Sessions, and J. C. Portal, Appl. Phys. Lett. 37, 178 (1980).
[16]H. Brendecke, H. L. Störmer, and R. J. Nelson, Appl. Phys. Lett. 35, 772 (1979).
[17]E. H. Perea, E. Mendez, and C. G. Fonstad, J. Electron. Mater. 9, 459 (1980).
[18]A. Pinczuk, J. M. Worlock, R. E. Nahory, and M. A. Pollack, Appl. Phys. Lett. 33, 461 (1978).
[19]G. M. Zinger, M. A. Il'in, E. P. Rashevskaya, and A. I. Ryskin, Fiz. Tverd. Tela 21, 2647 (1979) [Sov. Phys.—Solid State 21, 1522 (1979)].
[20]P. M. Amirtharaj, G. D. Holah, and S. Perkowitz, Phys. Rev. B 21, 5656 (1980).
[21]S. M. Kelso, D. E. Aspnes, C. G. Olson, D. W. Lynch, R. E. Nahory, and M. A. Pollack, in Proceedings of the Fourth International Conference on Ternary and Multinary Compounds, Tokyo, 1980 [Jpn. J. Appl. Phys. 19, Suppl. 19-3, 327 (1980)].
[22]K. Y. Cheng, A. Y. Cho, S. B. Christman, T. P. Pearsall, and J. E. Rowe, Appl. Phys. Lett. 40, 423 (1982).
[23]H. Burkhard, H. W. Dinges, and E. Kuphal, J. Appl. Phys. 53, 655 (1982).
[24]G. D. Henshall, P. D. Greene, G. H. B. Thompson, and P. R. Selway, Electron. Lett. 14, 796 (1978).
[25]H. Kawanishi, Y. Suematsu, Y. Itaya, and S. Arai, Jpn. J. Appl. Phys. 17, 1439 (1978).
[26]G. H. Olsen, C. J. Nuese, and M. Ettenberg, Appl. Phys. Lett. 34, 262 (1979).
[27]E. Oomura, T. Murotani, M. Ishii, and W. Susaki, Jpn. J. Appl. Phys. 18, 855 (1979).
[28]P. Chandra, L. A. Coldren, and K. E. Strege, Electron. Lett. 17, 6 (1981).
[29]A.-B. Chen and A. Sher, Phys. Rev. B 19, 3057 (1979).
[30]L. Fen and Z. Keiming, Chinese J. Semicond. 1, 257 (1980).
[31]V. L. Panyutin, B. E. Pondel'nikov, A. E. Rozenson, and V. I. Chizhikov, Fiz. Tekh. Poluprovodn. 14, 1000 (1980) [Sov. Phys.—Semicond. 14, 594 (1980)].
[32]A. preliminary and much abbreviated report is included in Ref. 21.
[33]D. E. Aspnes and A. A. Studna, Phys. Rev. B (in press).
[34]J. A. Van Vechten and T. K. Bergstresser, Phys. Rev. B 1, 3351 (1970).
[35]J. A. Van Vechten, O. Berolo, and J. C. Woolley, Phys. Rev. Lett. 29, 1400 (1972).
[36]M. A. Pollack, R. E. Nahory, J. C. DeWinter and A. A. Ballman, Appl. Phys. Lett. 33, 314 (1978).
[37]S. M. Kelso and D. E. Aspnes, unpublished data.
[38]D. E. Aspnes and A. A. Studna, Appl. Opt. 14, 220 (1974); Rev. Sci. Instrum. 49, 291 (1978).
[39]D. E. Aspnes, J. Vac. Sci. Technol. 17, 1057 (1980).
[40]D. E. Aspnes and A. A. Studna, Appl. Phys. Lett. 39, 316 (1981).
[41]D. E. Aspnes, Surf. Sci. 37, 418 (1973).
[42]D. E. Aspnes, J. Vac. Sci. Technol. 18, 289 (1981).
[43]E. O. Kane, Phys. Rev. 175, 1039 (1968).
[44]M. Cardona, Phys. Rev. B 15, 5999 (1977).
[45]D. E. Aspnes and M. Cardona, Solid State Commun. 27, 397 (1978).
[46]A. Daunois and D. E. Aspnes, Phys. Rev. B 18, 1824 (1978).
[47]S. E. Stokowski and D. D. Sell, Phys. Rev. B 5, 1636 (1972).
[48]A. Savitzky and M. J. E. Golay, Anal. Chem. 36, 1627 (1964); some errors in the original reference were corrected in J. Steinier, Y. Termonia, and J. Deltour,

Anal. Chem. 44, 1909 (1972).
[49]D. E. Aspnes, Phys. Rev. Lett. 28, 168 (1972).
[50]E. S. Keeping, *Introduction to Statistical Inference* (Van Nostrand, Princeton, 1962), Chap. 12.
[51]D. E. Aspnes and J. E. Rowe, Phys. Rev. Lett. 27, 188 (1971).
[52]J. Humlicek and E. Schmidt, Phys. Status Solidi B 107, K105 (1981).
[53]Y. Toyozawa, M. Inoue, T. Inui, M. Okazaki, and E. Hanamura, J. Phys. Soc. Jpn. 22, 1337 (1967).
[54]J. E. Rowe and D. E. Aspnes, Phys. Rev. Lett. 25, 162 (1970); 25, 979(E) (1970).
[55]D. E. Aspnes and J. E. Rowe, Phys. Rev. B 7, 887 (1973).
[56]K. L. Shaklee, J. E. Rowe, and M. Cardona, Phys. Rev. 174, 828 (1968).
[57]M. L. Cohen and T. K. Bergstresser, Phys. Rev. 141, 789 (1966).
[58]K. C. Pandey and J. C. Phillips, Phys. Rev. B 9, 1552 (1974).
[59]J. R. Chelikowsky and M. L. Cohen, Phys. Rev. B 14, 556 (1976).
[60]D. E. Aspnes and J. E. Rowe, in *Proceedings of the Tenth International Conference on the Physics of Semiconductors, Cambridge, 1970,* edited by S. P. Keller, J. C. Hensel, and F. Stern (U.S. AEC Dir. Tech. Information, Oak Ridge, Tenn. 1970), p. 442.
[61]M. Cardona, in *Atomic Structure and Properties of Solids,* edited by E. Burstein (Academic, New York, 1972).
[62]L. J. Sham, in Proceedings of the Fifteenth International Conference on the Physics of Semiconductors, Kyoto, 1980 [J. Phys. Soc. Jpn. 49, Suppl. A, 69 (1980)], and references therein.
[63]L. G. Suslina, A. G. Plyukhin, D. L. Fedorov, and A. G. Areshkin, Fiz. Tekh. Poluprovodn. 12, 2238 (1978) [Sov. Phys.—Semicond. 12, 1331 (1978)].
[64]S. D. Baranovskii and A. L. Éfros, Fiz. Tekh. Poluprovodn. 12, 2233 (1978) [Sov. Phys.—Semicond. 12, 1328 (1978)].
[65]D. Hennig and R. Strehlow, Phys. Status Solidi 107, 283 (1981).
[66]S. Sakai and T. Sugano, J. Appl. Phys. 50, 4143 (1979).
[67]M. Cardona, K. L. Shaklee, and F. H. Pollak, Phys. Rev. 154, 696 (1967).
[68]C. Varea de Alvarez, J. P. Walter, M. L. Cohen, J. Stokes, and Y. R. Shen, Phys. Rev. B 6, 1412 (1972).
[69]M. Welkowsky and R. Braunstein, Phys. Rev. B 5, 497 (1972).
[70]E. W. Williams and V. Rehn, Phys. Rev. 172, 798 (1968); Solid State Commun. 7, 545 (1969).
[71]A. G. Thompson and J. C. Woolley, Can. J. Phys. 45, 2597 (1967); C. C. Y. Kwan, A. G. Thompson, and J. C. Woolley, *ibid.* 46, 2733 (1968).
[72]A. G. Thompson and J. C. Woolley, Can. J. Phys. 45, 255 (1967).
[73]S. S. Vishnubhatla, B. Eyglunent, and J. C. Woolley, Can. J. Phys. 47, 1661 (1969).
[74]R. L. Moon, G. A. Antypas, and L. W. James, J. Electron. Mater. 3, 635 (1974).
[75]D. Stroud, Phys. Rev. B 5, 3366 (1972).
[76]R. Hill, J. Phys. C 7, 521 (1974).
[77]M. Altarelli, Solid State Commun. 15, 1607 (1974).
[78]A.-B. Chen and A. Sher, Phys. Rev. Lett. 40, 900 (1978); Phys. Rev. B 17, 4726 (1978).
[79]T. P. Pearsall, in Ref. 2, Chap. 12.
[80]The Van Vechten—Bergstresser approach (Ref. 34) is appropriate for the *average* $E_1$ gap, i.e., $\frac{1}{3}[2E_0+(E_0+\Delta_0)]$. However, as can be seen from Table I, the bowing parameter for this gap, 0.31 eV, is still larger than the calculation gives, 0.15 eV.
[81]O. Berolo and J. C. Woolley, in *Proceedings of the 11th International Conference on the Physics of Semiconductors, Warsaw, 1972* (Polish Scientific, Warsaw, 1972), p. 1420.
[82]C. Alibert, G. Bordure, A. Laugier, and J. Chevallier, Phys. Rev. B 6, 1301 (1972).
[83]D. J. Chadi, Phys. Rev. B 16, 790 (1977).
[84]M. Cardona and D. L. Greenaway, Phys. Rev. 125, 1291 (1962).
[85]D. E. Aspnes, Phys. Rev. Lett. 28, 913 (1972).
[86]D. E. Aspnes, Phys. Rev. B 12, 2297 (1975).
[87]D. E. Aspnes and A. A. Studna, Phys. Rev. B 7, 4605 (1973).
[88]In zinc-blende materials, the critical point is very slightly displaced from $\Gamma$ in the $\langle 111 \rangle$ direction due to a small $k$-linear term (unrelated to the other one we have been discussing here) arising from the lack of inversion symmetry. This effect is expected to be very small and will be neglected in this paper. See E. O. Kane, J. Phys. Chem. Solids 1, 249 (1956).
[89]R. R. L. Zucca and Y. R. Shen, Phys. Rev B 1, 2668 (1970).
[90]J. E. Fischer, in *Proceedings of the Tenth International Conference on the Physics of Semiconductors, Cambridge, 1970,* edited by S. P. Keller, J. C. Hensel, and F. Stern (U.S. AEC Dir. Tech. Information, Oak Ridge, Tenn., 1970), p. 427; T. M. Donovan, J. E. Fischer, J. Matsuzaki, and W. E. Spicer, Phys. Rev. B 3, 4292 (1971).
[91]D. D. Sell and E. O. Kane, Phys. Rev. B 5, 417 (1972).
[92]The atomic spin-orbit splittings are renormalized in solids. See Ref. 83.
[93]M. Cardona, *Modulation Spectroscopy* (Academic, New York, 1969), p. 242; private communication.
[94]The appropriate analysis is analogous to that given for $\Delta_0$ in Ref. 83.